

IS THE COSMOS TRANSPARENT?

Mahid Anjum

Supervised by Anastasios Avgoustidis

Assuming flat Λ CDM cosmology, supernovae and $H(z)$ (expansion rate of the universe) data are analyzed to find out ‘How transparent is the cosmos?’. By considering how distances are affected in a non-transparent universe and combining analysis of supernovae with analysis of cosmic expansion rate measurements, the parameter ϵ , which encodes departures from a transparent universe, is constrained. The resulting constraints put on ϵ are shown in figure 7. It is found that $\epsilon \sim -0.02$, or more coarsely, lies in the range $-0.06 \lesssim \epsilon \lesssim 0.04$ (3σ). These findings support a transparent universe (negligible opacity). The amount of matter (ordinary and dark) and dark energy in the current epoch are also determined. This is done by constraining the mass density parameter Ω_m using supernovae data. The following results are obtained: $\Omega_m = 0.276^{+0.061}_{-0.050}$ (99.73% confidence), or equivalently $\Omega_\Lambda = 0.724$. These results imply the universe today is dominated by dark energy (72%) whereas matter makes up the remaining 28%.

CONTENTS

I	Introduction	1
I.i	Distances in cosmology & The Hubble parameter	1
I.ii	Why SNe Ia?	2
I.iii	Aims	3
II	Method & Results	4
II.i	Constraining best-fit parameter(s)	4
II.ii	Constraining opacity	7
III	Conclusions & Discussion	9
	References	11
	Appendix	12

I INTRODUCTION

In the late 1990s, two teams published their findings on Type Ia supernovae (SNe Ia) which later proved to be seminal for our understanding of the universe. Observational evidence suggested that high-redshift SNe Ia were fainter than expected [1, 2]. This discrepancy was interpreted as evidence for an accelerated expansion of the universe.

However, numerous other phenomena which could bring about supernovae dimming, similar to as that caused by an accelerated expansion of the universe, were explored. For e.g., [3] presents a model in which photons could be converted into axions (dark matter candidate) while traversing the intergalactic medium. This means if the number of photons is not conserved, i.e., some photons are lost on their way to the observer, then the source (for e.g., a supernova) appears to be at a distance further than the true distance, hence mimicking an expanding universe (see section I.i).

The primary aim of this study is to constrain a possible “degree of opaqueness” of the universe, more aptly termed, “cosmic opacity (τ)”, by considering possible deviations from a completely transparent universe. However, before delving in how exactly this study aims to accomplish this, it deems appropriate to define cosmological quantities relevant to this study and briefly explore why SNe Ia are so ubiquitous in observational cosmology.

I.i Distances in cosmology & The Hubble parameter

“Luminosity distance (d_{lum})” is defined as the distance an object appears to have, assuming the inverse square law holds [4]. It’s mathematically defined as:

$$d_{\text{lum}} = \sqrt{\frac{L}{4\pi f}}, \quad (1)$$

where L denotes the luminosity of the object and f is the flux of photons measured. If geometry of the universe is flat, as suggested by the WMAP mission [5], then luminosity distance can be calculated as [6]:

$$d_{\text{lum}}(z) = c(1+z) \int_0^z \frac{dz'}{H(z')}, \quad (2)$$

where c is the speed of light, z denotes redshift and $H(z)$ is the Hubble parameter (expansion rate of the universe). d_{lum} is sensitive to photon conservation, i.e., if photons are lost on their way to the observer then the observed luminosity distance is greater than the true (“would be”) luminosity distance if photon conservation were to hold. An increase in luminosity distance is analogous to the object appearing dimmer to the observer.

Supernovae datasets are often presented in terms of “distance modulus (μ)”, which is related to d_{lum} , as follows [6]:

$$\mu = m - M = 5 \log(d_{\text{lum}}(\text{Mpc})) + 25, \quad (3)$$

where m denotes the apparent magnitude and M denotes the absolute magnitude of the object.

Another important distance measure in observational cosmology is the “angular diameter distance (d_A)”. It is defined as the distance an object of known physical extent appears to be at, assuming Euclidean geometry [4]. It is related to the luminosity distance by the simple “Etherington relation” [7, 8]:

$$d_{\text{lum}} = (1+z)^2 d_A. \quad (4)$$

It is important to note at this point that $H(z)$ and d_A measurements are insensitive to photon conservation. However, equation (4) doesn’t hold true if photon conservation is violated [8].

In Λ CDM cosmology, the only constituents of the universe are matter and a cosmological constant Λ (often associated with dark energy), this implies that:

$$\Omega_m + \Omega_\Lambda = 1, \quad (5)$$

for a flat universe consisting only of matter and Λ [4]. In equation (5), Ω_m denotes the matter density parameter and Ω_Λ denotes the cosmological constant density parameter. Under these considerations (flat Λ CDM model), the Hubble parameter, $H(z)$, can be written as [6]:

$$\begin{aligned} H(z) &= H_0 \sqrt{\Omega_m(1+z)^3 + \Omega_\Lambda}, \\ &= H_0 \sqrt{\Omega_m(1+z)^3 + (1 - \Omega_m)}, \end{aligned} \quad (6)$$

where equation (5) has been used to rewrite $H(z)$ in terms of H_0 , Ω_m and z . H_0 is the Hubble constant (present-day value of Hubble parameter). Now we can proceed to investigating what's so special about SNe Ia that makes them so useful in observational cosmology.

I.ii Why SNe Ia?

Supernovae are stellar explosions typically occurring when a massive star nears the end of its lifetime or when a non-rotating white dwarf's mass grows beyond the "Chandrasekhar mass ($\approx 1.44M_\odot$)" [9]. These explosions are extremely luminous and can briefly outshine the host galaxy.



Figure 1: **Left:** Remnant from Tycho supernova (type Ia). Red corresponds to low energy x-rays whereas blue corresponds to high energy x-rays. **Middle:** SN 1994D (bright spot on the lower left), another type Ia supernova. **Right:** Supernova remnant SNR E0519-69.0 in the Large Magellanic Cloud. CC: [NASA/ESA](#).

Specifically, type Ia supernovae occur when mass accretion from a binary companion causes the explosion of a white dwarf. SNe Ia are classified based on the fact that their spectra are dominated by lines from higher-mass elements like calcium, sulphur, silicon and iron, but lack hydrogen and helium [9]. The use of SNe Ia in observational cosmology is underpinned by the fact that they “almost” have the same peak absolute magnitude, M_{peak} [4]. The word “almost” was used because in reality there exists a correlation between the peak absolute magnitude and the rate at which these supernovae fade [10, 11]. For this reason, SNe Ia are referred to as “standardisable candles” rather than standard candles [4, 9]. Since the corresponding peak apparent magnitude, m_{peak} , can be observed, and there exist astronomical techniques to estimate M_{peak} , equation (3) can be utilized to calculate distances to these objects. This explains the utility of SNe Ia as “distance indicators” in observational cosmology¹.

¹For a detailed discussion of supernovae physics and their use in observational cosmology, refer to [9].

I.iii Aims

The Supernova Cosmology Project (SCP) union2.1 SNe Ia compilation [12] provides distance modulus data for 580 SNe Ia over the redshift interval [0.015, 1.414]. Figure 2 shows both μ and d_{lum} for the observed SNe Ia as functions of redshift.

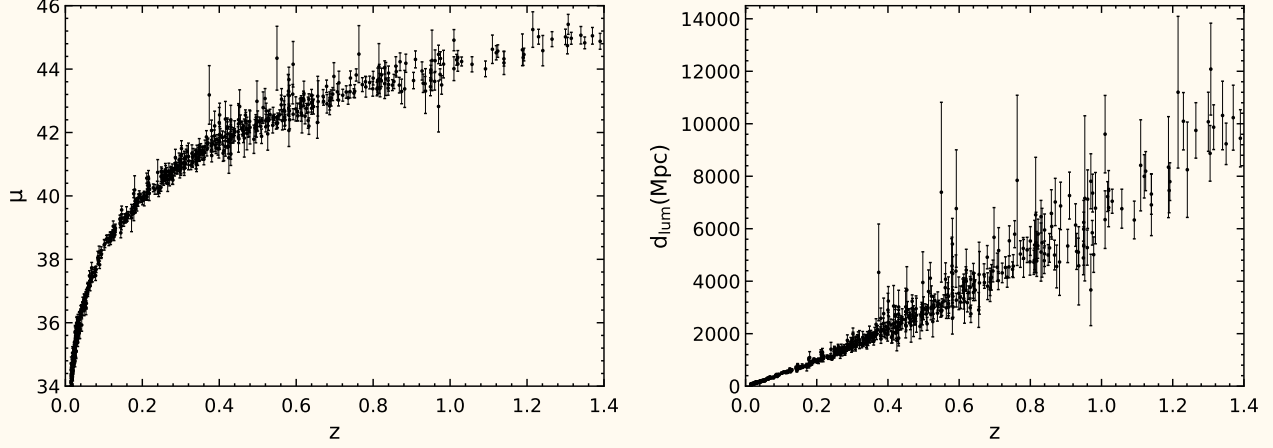


Figure 2: **Left:** The distance moduli, μ , of SNe Ia plotted as functions of redshift. Distance moduli data (with uncertainties) was obtained from union2.1 compilation of the SCP [12]. **Right:** The corresponding luminosity distances, d_{lum} , of the supernovae plotted as functions of redshift z . Equation (3) was used to convert SNe Ia distance moduli, μ , into luminosity distances, d_{lum} . Presuming error calculations for d_{lum} are correct (see equation (7)), it can be inferred that luminosity distances of high-redshift SNe Ia have greater uncertainties. This hints at the fact that it gets increasingly difficult to obtain accurate distance measurements of distant astronomical objects. Uncertainties in redshift were not provided since spectroscopic measurements of redshift are extremely accurate.

Since SNe Ia data being used is in terms of μ , equation (3) has been utilized to convert μ to d_{lum} (in Mpc). Error propagation has been carried out to compute the uncertainty in luminosity distances, denoted δd_{lum} , using equation (7)²:

$$\delta d_{lum} = d_{lum} \left(\frac{\ln 10}{5} \right) \cdot \delta \mu, \quad (7)$$

where $\delta \mu$ is the uncertainty in observed distance modulus for SNe Ia given by [12].

1st part of the study is concerned with finding the value of Ω_m that best fits SNe Ia data for μ and d_{lum} (displayed in figure 2). This can be accomplished via the χ^2 -minimization routine suggested in [13]. Main steps of the routine are displayed in figure 3. In essence, χ^2 is a manifestation of the “least squares method” and can be described as a “merit function” which quantifies disagreement between a physical model and the observed data. It is mathematically defined as [13]:

$$\chi^2 = \sum_i \left\{ \frac{[D_i - y(x_i|\Theta)]^2}{\sigma_i^2} \right\}, \quad (8)$$

where D_i denotes the observed data points, σ_i denotes the corresponding uncertainty in the i -th observed data point and $y(x_i|\Theta)$ is a model function characterized by parameter(s) Θ . Practically, one wants minimal disagreement between observed data and the proposed physical model, i.e., minimum χ^2 (minimum disagreement). The specific parameter(s) Θ for which χ^2 is minimized are referred to as “best-fit parameter(s)”. A useful χ^2 rule worth noting is: the minimum χ^2 , χ^2_{min} , should be close to the number of data points [13].

Numerous studies have previously used χ^2 -minimization to constraint cosmological parameters. For e.g., In [12], the authors used SNe Ia data and χ^2 -minimization to constrain Ω_m (assuming flat Λ CDM cosmology). However, one is not limited to using SNe Ia measurements only. Extending their study ([12]), the authors then

²Refer the [appendix](#) to see full derivation.

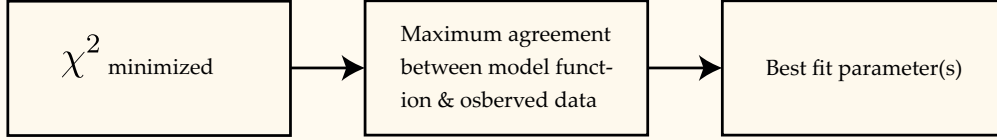


Figure 3: The χ^2 minimization routine from [13]. Using this routine one can fit a theoretical model to observed data. A minimized χ^2 corresponds to least disagreement between the model and data, and can be used to extract the best fit parameter(s).

utilize other measurements (H_0 , cosmic microwave background (CMB), baryon acoustic oscillations (BAO)) with SNe Ia measurements to put combined constraints on Ω_m . In [14], the authors constrain Ω_m 1st with BAO measurements alone and then with BAO & large-scale structure clustering measurements combined. Instead of using χ^2 , they opt for “likelihood functions”.

In the later part of the study, opacity (τ) is inducted into our analysis to investigate transparency of the universe. The following parameterization of opacity is considered [8]:

$$\tau(z) = 2\epsilon z, \quad (9)$$

where the parameter ϵ encodes possible deviations from a transparent universe. Any deviation from a transparent universe implies that several cosmological quantities (sensitive to photon conservation) would have to be redefined since the Etherington relation, $d_{lum}d_A^{-1} = (1+z)^2$, wouldn’t hold anymore in its current form. In fact, with ϵ considered, the Etherington relation is modified to : $d_{lum}d_A^{-1} = (1+z)^{2+\epsilon}$. Using $\epsilon = 0$ in this expression, one recovers the original Etherington relation (i.e., $\epsilon = 0$ corresponds to a completely transparent universe).

Combining SNe Ia measurements with Hubble parameter measurements from [15], this study aims to constrain ϵ . This would allow us to determine whether what we think of as cosmic acceleration is, in fact, the universe expanding and not a source of photon absorption (non-transparent universe) mimicking the expansion. Several studies have previously probed cosmic transparency. Similar to the approach opted in this study, [8] combines SNe Ia measurements with $H(z)$ measurements to constrain Ω_m and ϵ (assuming Λ CDM cosmology). However, a more robust approach is undertaken by authors of [16, 17, 18, 19]. In these studies, cosmological-model independent schemes are presented to constrain opacity. All of these studies utilize SNe Ia measurements in one way or another. For e.g., [16, 18] use SNe Ia & $H(z)$ measurements, [17] uses lensed & unlensed SNe Ia measurements and [19] uses SNe Ia & gravitational waves measurements.

II METHOD & RESULTS

II.i Constraining best-fit parameter(s)

To obtain best fit parameter(s) for SNe Ia data, a theoretical model for luminosity distance, d_{lum} , and distance modulus, μ , is needed. This is because computing χ^2 requires a theoretical model against which observed data can be compared. Assuming flat Λ CDM cosmology, the theoretical luminosity distance, denoted by d_{lum}^{theo} , can be calculated using equation (10), which has been derived by replacing $H(z')$ in equation (2) by its definition from equation (6):

$$d_{lum}^{theo}(z, \Omega_m) = \frac{c(1+z)}{H_0} \int_0^z \frac{dz'}{\sqrt{\Omega_m(1+z')^3 + (1-\Omega_m)}}. \quad (10)$$

Moving on, the theoretical distance modulus, μ_{theo} , can be obtained by substituting d_{lum}^{theo} in equation (3):

$$\mu_{theo}(z, \Omega_m) = 5 \log(d_{lum}^{theo}(z, \Omega_m)) + 25. \quad (11)$$

With theoretical distance models devised, d_{lum}^{theo} was computed by solving the integral in equation (10) using discretization. The integral was evaluated over equally-spaced arrays of z (range [0.01, 1.414])

and Ω_m (range $[0, 1]$). In other words, equation (10) was solved for each Ω_m over the same redshift interval $([0.01, 1.414])$. Note that for a fruitful computation of d_{lum}^{theo} a numerical value of H_0 is needed. The corresponding distance moduli, μ_{theo} , were then calculated using equation (11). Owing to processing power constraints, 200 values each of both redshift and Ω_m were considered in the aforementioned intervals. This implies that 200 different μ_{theo} vs z curves/relations were computed, each of which corresponded to a different Ω_m being used. These can be thought of as 200 different “toy universes”, each having its own μ_{theo} vs z relation. Three computations were carried out with H_0 set = 65, 70 and 74 $\text{kms}^{-1} \text{Mpc}^{-1}$. Figure 4 shows μ_{theo} as a function of redshift (H_0 set = 70 $\text{kms}^{-1} \text{Mpc}^{-1}$) for 5 such “toy universes” on top of SNe Ia data. In fact, what we are after is to determine which “toy universe” best fits the data obtained in the real universe.

Having both the observed and theoretical distance moduli at our disposal now, one χ^2 value each was calculated for every “toy universe” using equation (12):

$$\chi^2(\Omega_m) = \sum_i \left\{ \frac{[\mu_i^{obs} - \mu_i^{theo}(z_i, \Omega_m)]^2}{(\delta\mu_i^{obs})^2} \right\}, \quad (12)$$

where i “runs over” the observed SNe Ia data points and μ^{obs} and $\delta\mu^{obs}$ denote the observed SNe Ia distance moduli and the respective error, both of which were obtained from SNe Ia data. In other words, disagreement between each “toy universe” and the actual universe was quantified by comparing μ_{theo} of each “toy universe” against observed μ of SNe Ia. The minimum χ^2 , out of all χ^2 s computed, corresponds to the best fit through observed SNe Ia distance moduli data. Since χ^2 is a function of Ω_m (equation (12)), χ_{min}^2 corresponds to $(\Omega_m)_{best}$, the best-fit value of Ω_m (our theoretical model, μ_{theo} , is characterized by Ω_m). Table 1 shows χ_{min}^2 and $(\Omega_m)_{best}$ obtained with each value of H_0 used in our analysis.

$H_0 / \text{kms}^{-1} \text{Mpc}^{-1}$	χ_{min}^2	$(\Omega_m)_{best}(1\sigma)$	$(\Omega_m)_{best}(2\sigma)$	$(\Omega_m)_{best}(3\sigma)$
74.0	691	$0.141^{+0.010}_{-0.005}$	$0.141^{+0.015}_{-0.015}$	$0.141^{+0.030}_{-0.025}$
70.0	563	$0.281^{+0.010}_{-0.010}$	$0.281^{+0.021}_{-0.020}$	$0.281^{+0.041}_{-0.035}$
65.0	785	$0.553^{+0.015}_{-0.015}$	$0.553^{+0.025}_{-0.025}$	$0.553^{+0.050}_{-0.050}$

Table 1: Results obtained for χ_{min}^2 and $(\Omega_m)_{best}$ with H_0 values used in our analysis. 200 “toy universes” were considered for comparison against SNe Ia data (figure 2), each having a different value of Ω_m from the interval $[0, 1]$. Ω_m confidence intervals were determined by 1st determining χ^2 confidence levels using single parameter $\delta\chi^2$ ($\chi^2 - \chi_{min}^2$) values given in [13], and then finding out which values of Ω_m lie in each confidence region.

From table 1 it can be seen that χ_{min}^2 , and consequently $(\Omega_m)_{best}$, are sensitive to the value of H_0 used in our computation of μ_{theo} and d_{lum}^{theo} . Since we are interested in determining the best-fit value for Ω_m , we would like to make our χ_{min}^2 computation insensitive to the value of H_0 used. In other words, we would like to determine $(\Omega_m)_{best}$ regardless of the value of H_0 input. This allows us to get rid of the H_0 bias present in our analysis hitherto. This is referred to as “marginalization over H_0 ” [13]. We marginalize over H_0 indirectly by considering different “theoretical” absolute magnitudes (intrinsic brightnesses) of SNe Ia in our computation of μ_{theo} . This is analogous to considering different values of H_0 . With different theoretical absolute magnitudes included in μ_{theo} , equation (11) is “updated” to:

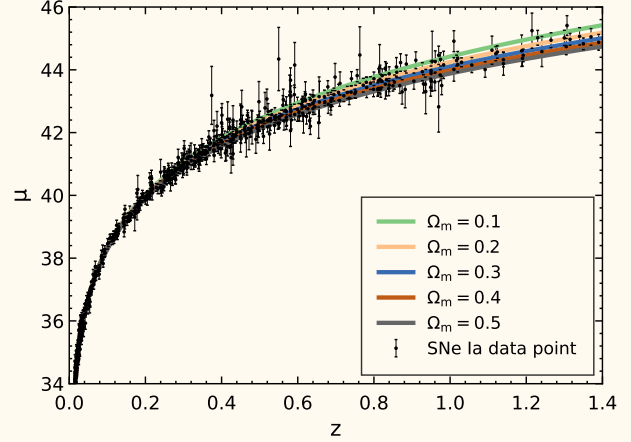


Figure 4: Five different μ_{theo} are plotted as functions of redshift z on top of the SNe Ia distance moduli. As can be seen in the plot, each μ_{theo} corresponds to a different value of Ω_m being used in the calculation. These can be thought of as 5 different “toy universes” in comparison against the actual universe (observed SNe Ia data). $H_0 = 70 \text{ kms}^{-1} \text{Mpc}^{-1}$ was used in this case.

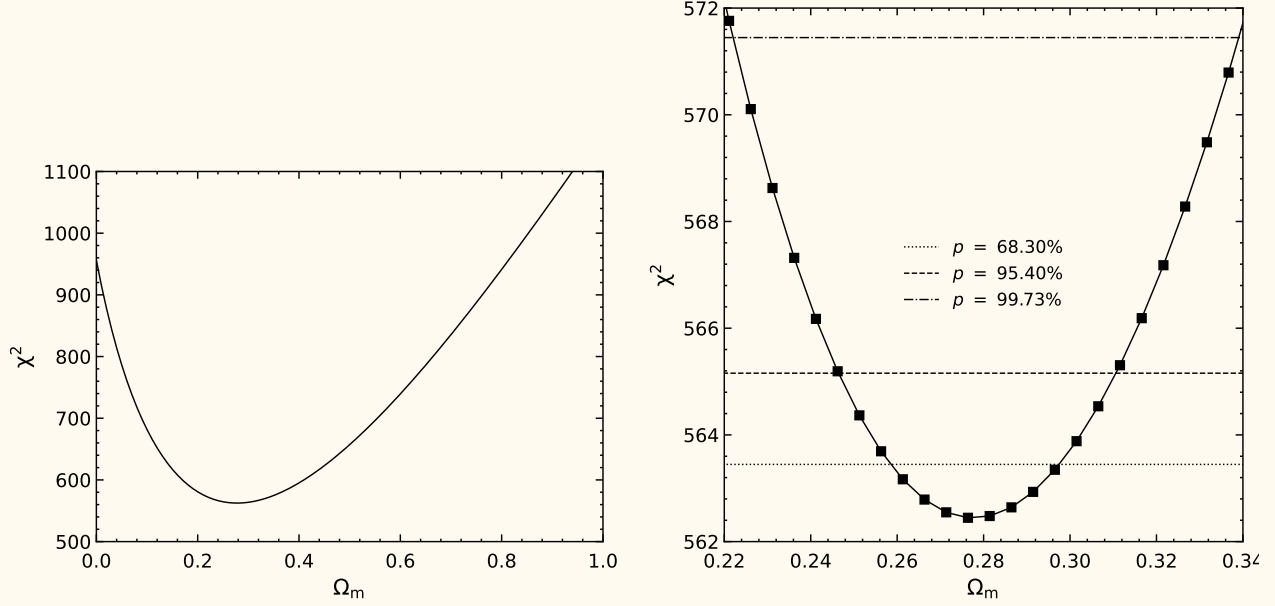


Figure 5: χ^2 as a function of Ω_m having marginalized over H_0 indirectly. 200 “toy universes” were considered for comparison against SNe Ia data (figure 2), each having a different value of Ω_m from the interval $[0, 1]$. **Right:** χ^2 values satisfying the inequality $\delta\chi^2 \leq 10$ are shown on the vertical axis. Dotted line corresponds to 1σ confidence level ($\delta\chi^2 = 1.00$), dashed line corresponds to 2σ confidence level ($\delta\chi^2 = 2.71$) and dash-dotted line corresponds to 3σ confidence level ($\delta\chi^2 = 9.00$). p represents the confidence percentages. In this case, same values of χ^2_{\min} and $(\Omega_m)_{\text{best}}$ are obtained no matter what value of H_0 is used in our analysis (as long as the same value of H_0 is used in computing $d_{\text{lum}}^{\text{theo}}$ (equation (10)) and M_{theo} (equation (14))). $\delta\chi^2$ values for each confidence level were obtained from Table 1 in [13]. As can be seen from the plot χ^2 is minimized around $\Omega_m \approx 0.28$. Flat Λ CDM cosmology was assumed.

$$\mu_{\text{theo}}(z, \Omega_m) = 5 \log(d_{\text{lum}}^{\text{theo}}(z, \Omega_m)) + M_{\text{theo}}(\Omega_m), \quad (13)$$

where M_{theo} denotes the theoretical absolute magnitude which itself was determined (for each Ω_m) using equation (14):

$$M_{\text{theo}}(\Omega_m) = \frac{\sum_i \left\{ \frac{\mu_{\text{obs}}(z_i) - 5 \log[d_{\text{lum}}^{\text{theo}}(z_i, \Omega_m)]}{\delta\mu_{\text{obs}}(z_i)^2} \right\}}{\sum_i \left\{ \frac{1}{\delta\mu_{\text{obs}}(z_i)^2} \right\}}, \quad (14)$$

where i “runs over” the observed SNe Ia data points. M_{theo} for each Ω_m was computed using redshift values of SNe Ia from [12]. Once M_{theo} had been determined for each of our “toy universes”, μ_{theo} were calculated using equation (13). At this point we had all the ingredients required for computing χ^2 , hence in the next step, χ^2 was calculated for each “toy universe” by comparing the respective μ_{theo} against observed μ from SNe Ia data. As pointed out earlier, the minimum χ^2 , out of all the χ^2 computed, corresponds to best-fit Ω_m .

The results obtained with (indirect) marginalization over H_0 for χ^2_{\min} and $(\Omega_m)_{\text{best}}$ are tabulated in table 2. Figure 5 shows χ^2 as a function of Ω_m . χ^2 confidence levels shown in figure 5 were determined using $\delta\chi^2$ values given in Table 1 of [13], here $\delta\chi^2 = \chi^2 - \chi^2_{\min}$. In this case, the single parameter values of $\delta\chi^2$ from [13] were used since χ^2 is a function of Ω_m only. These confidence levels allowed us to determine the corresponding values of Ω_m lying in each confidence region, which in turn allowed us to place constraints around $(\Omega_m)_{\text{best}}$ displayed in tables 1 and 2. Note the “gaps” between (Ω_m, χ^2) data points shown in figure 5 (right). These are due to the fact that only 200 values of Ω_m between 0 & 1 were used for μ_{theo} and χ^2 computations. Which meant the constraints placed around $(\Omega_m)_{\text{best}}$ would not come out to be extremely precise since errors in each confidence interval (1σ , 2σ or 3σ) are varying in steps of 0.005. This is not a coincidence because $0.005 \left(\frac{1-0}{200}\right)$ is exactly the step size between each Ω_m value considered in our analysis.

χ^2_{\min}	$(\Omega_m)_{\text{best}}(1\sigma)$	$(\Omega_m)_{\text{best}}(2\sigma)$	$(\Omega_m)_{\text{best}}(3\sigma)$
562(.447)	$0.276^{+0.020}_{-0.015}$	$0.276^{+0.031}_{-0.025}$	$0.276^{+0.061}_{-0.050}$

Table 2: χ^2_{\min} and $(\Omega_m)_{\text{best}}$ having marginalized over H_0 indirectly. 200 “toy universes” were considered for comparison against SNe Ia data (figure 2), each having a different value of Ω_m from the interval $[0, 1]$. The uncertainties around $(\Omega_m)_{\text{best}}$ were calculated by 1st determining χ^2 confidence levels using single parameter $\delta\chi^2$ values given in [13] and then finding out corresponding values of Ω_m lying in each of these confidence regions.

In calculating χ^2 , a problem was faced that needs to be mentioned. From equation (12), it can be inferred that we need to calculate μ_{theo} at very specific redshifts (redshifts of the observed SNe Ia data (580 values & not equally-spaced)), while we have calculated it on an array of 200 equally-spaced redshift values, which aren’t the same as data redshifts. This problem was tackled using “interpolation”. In a nutshell, interpolation uses existing values to estimate a function at unknown values, essentially “filling gaps” in between the existing data points. Figure 6 shows two different types of interpolation for some “dummy data”. In our analysis, μ_{theo} was interpolated using “cubic” interpolation over data redshift values of observed SNe Ia.

II.ii Constraining opacity

We now proceed towards constraining opacity (τ) so that transparency of the universe can be studied. The following parameterization of opacity is considered in our modelling: $\tau = 2\epsilon z$ (see equation (9)). In reality, there are sources of attenuation or brightening (gray dust & gravitational lensing etc.) which could alter the number of photons received from a source [19] and mimic a non-transparent universe.

In a opaque or non-transparent universe, the flux of photons received from the source supernovae would be attenuated by a factor of $e^{-\tau(z)}$. This implies the observed luminosity distance is now:

$$(d_{\text{lum}}^{\text{obs}})^2 = (d_{\text{lum}}^{\text{true}})^2 \cdot e^{\tau(z)}. \quad (15)$$

Where $d_{\text{lum}}^{\text{true}}$ denotes the observed luminosity distance in a completely transparent universe ($\epsilon = 0$, photon-conservation holds). Substituting for $d_{\text{lum}}^{\text{obs}}$ in equation (3) lets us devise the effect on observed distance modulus:

$$\mu_{\text{obs}}(z) = \mu_{\text{true}}(z) + 2.5 \log(e) \cdot \tau(z), \quad (16)$$

where $\mu_{\text{true}} = 5 \log(d_{\text{lum}}^{\text{true}}) + 25$ and μ_{obs} is the observed distance modulus. This means the theoretical distance modulus, μ_{theo} , is now a function of redshift, Ω_m and ϵ :

$$\mu_{\text{theo}}(z, \Omega_m, \epsilon) = 5 \log(d_{\text{lum}}^{\text{theo}}(z, \Omega_m)) + M_{\text{theo}}(\Omega_m, \epsilon) + 2.5 \log(e) \cdot 2\epsilon z, \quad (17)$$

where we have considered different theoretical absolute magnitudes (M_{theo}) of supernovae to indirectly marginalize over H_0 , as done in the previous section.

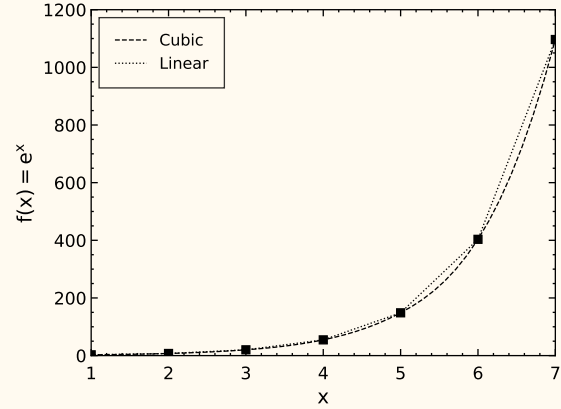


Figure 6: Different types of interpolation performed for “dummy” data generated in Python. It can be seen that our data function, $f(x)$, has “gaps” in between the data points. Two types of interpolation have been performed to “fill in” the gaps over which $f(x)$ was originally unknown. Having performed interpolation, one can estimate $f(x)$ over the complete x interval $[0, 7]$. As can be seen from the plot, cubic interpolation connects the data much more smoothly than linear interpolation and hence is a more viable choice in most cases.

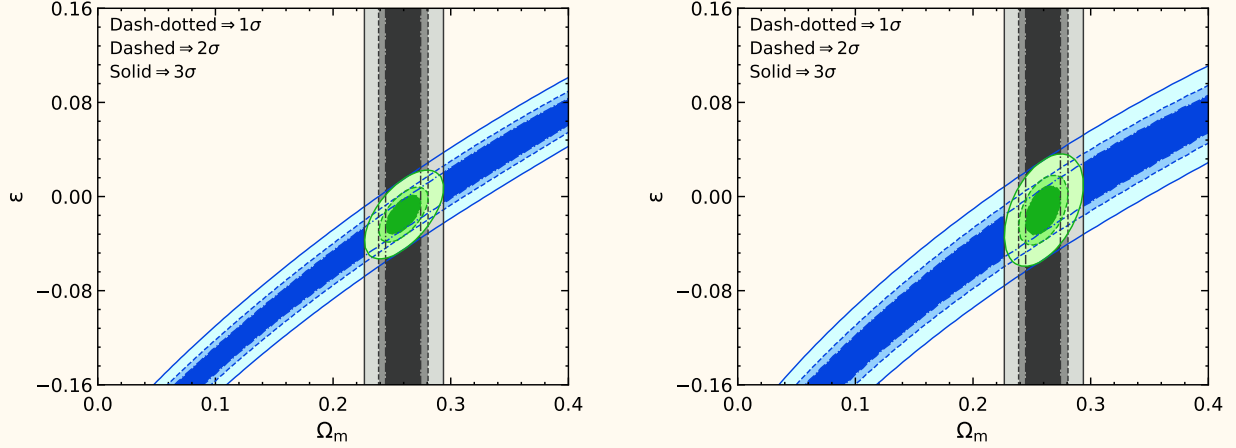


Figure 7: Shows constraints/confidence levels (1σ (dash-dotted, $\delta\chi^2 = 2.30$), 2σ (dashed, $\delta\chi^2 = 4.61$) and 3σ (solid, $\delta\chi^2 = 11.8$)) put on Ω_m and ϵ by analysis of SNe Ia (blue), $H(z)$ (grey) and combined (green). The confidence region boundaries in each case were determined using two parameter $\delta\chi^2$ values given in **Table 1** of [13]. **Left:** In this case, no marginalization over H_0 was carried out in the analysis for SNe Ia and $H(z)$. **Right:** In this case, marginalization over H_0 was carried out in the analysis of SNe Ia but not $H(z)$. Flat Λ CDM cosmology was assumed.

In this case, M_{theo} were calculated using equation (18):

$$M_{\text{theo}}(\Omega_m, \epsilon) = \frac{\sum_i \left\{ \frac{\mu_{\text{obs}}(z_i) - 5 \log [d_{\text{lum}}^{\text{theo}}(z_i, \Omega_m)] - 2.5 \log(e) \cdot 2\epsilon z_i}{\delta\mu_{\text{obs}}(z_i)^2} \right\}}{\sum_i \left\{ \frac{1}{\delta\mu_{\text{obs}}(z_i)^2} \right\}} \quad (18)$$

where, as previously, i “runs over” the observed SNe Ia data points. 200 equally-spaced values of Ω_m and ϵ were considered over the intervals $[0, 1]$ and $[-1, 1]$, respectively, with redshifts of SNe Ia data. For the computation of μ_{theo} , 200 equally-spaced values of redshift were used over the interval $[0.01, 1.414]$ with Ω_m and ϵ intervals staying the same.

Once theoretical distance moduli, μ_{theo} , had been calculated using equation (17), χ^2 calculations were performed based on equation (12). Note that in this case χ^2 is a function of both Ω_m and ϵ , i.e., $\chi^2(\Omega_m, \epsilon)$, because μ_{theo} is a function of z , Ω_m and ϵ (see equation (18)). Once again, interpolation was utilized to estimate μ_{theo} at the “gaps” in our “artificial” redshift range. This was done because the sum in equation (12) is to be computed at specific redshifts of SNe Ia data which are not equally-spaced and are greater in number than “artificial” redshifts considered in our analysis.

As mentioned in section I.iii, we expect to put combined (SNe Ia + $H(z)$) constraints on ϵ . This is simply because luminosity distance measurements from SNe Ia are sensitive to photon conservation whereas $H(z)$ measurements are not. Since χ^2 calculations for SNe Ia had been performed by this point, the next step was computing χ^2 for $H(z)$ measurements.

$H(z)$ data (with errors) utilized in this study was obtained from **Table 1** in [15]. Theoretically-expected values of $H(z)$, denoted by $H_{\text{theo}}(z, \Omega_m)$, were calculated (with $H_0 = 70 \text{ km s}^{-1} \text{ Mpc}^{-1}$) by evaluating equation (6) at redshifts of $H(z)$ data. As previously, 200 equally-spaced Ω_m values were considered in the interval $[0, 1]$. Once we had both data and theoretically-expected values for $H(z)$, χ^2 calculations, based on equation (8), were carried out. In calculating $\chi^2(\Omega_m)$ for $H(z)$, interpolation wasn’t implemented since H_{theo} calculations performed earlier were exactly at $H(z)$ data redshifts. Marginalization over H_0 wasn’t carried out.

Having performed χ^2 calculations for both SNe Ia and $H(z)$, the combined χ^2 were obtained using equation (19):

$$\chi_{\text{combined}}^2(\Omega_m, \epsilon) = \chi_{\text{SN}}^2(\Omega_m, \epsilon) + \chi_{H(z)}^2(\Omega_m). \quad (19)$$

Since $\chi^2_{H(z)}$ depends only on Ω_m (1D), its addition with χ^2_{SNe} (2D) was made possible by trivially copying the 1D array across the 2nd dimension so that it could be plotted on the $\epsilon - \Omega_m$ plane (χ^2 is a 2D-function in this case). Figure 7 shows the resulting constraints (confidence regions) put on ϵ and Ω_m by analysis of SNe Ia, $H(z)$ and both combined. More specifically, **(left)** shows constraints when SNe Ia analysis was carried out without marginalizing over H_0 , i.e., M_{theo} was set = 25 in equation (17) and a value of $70 \text{ kms}^{-1} \text{ Mpc}^{-1}$ was used for H_0 in computing μ_{theo} . **(right)** shows constraints by SNe Ia analysis with marginalization over H_0 . Confidence regions (1σ , 2σ and 3σ) for SNe Ia, $H(z)$ and combined shown in figure 7 were determined using $\delta\chi^2$ values given in Table 1 of [13]. In this case, two parameter values of $\delta\chi^2$ were used since χ^2 was now a function of Ω_m and ϵ .

However, there is a caveat here that can be overlooked. In the case of $H(z)$, χ^2 is, in fact, not a function of two but one parameter (Ω_m), then, why were two parameter $\delta\chi^2$ values used in determining the confidence region boundaries? The line of reasoning goes as follows: since we had to project the confidence regions on a two parameter plane (ϵ, Ω_m), that is why two parameter $\delta\chi^2$ values from [13] were used.

III CONCLUSIONS & DISCUSSION

Distance moduli data obtained from the union 2.1 SNe Ia compilation were compared against predicted distance moduli (within flat Λ CDM cosmology) by the virtue of χ^2 function. Minimizing χ^2 , the best-fit value of Ω_m was obtained to be $0.276^{+0.061}_{-0.050}$ (99.73% confidence), or equivalently $\Omega_\Lambda = 0.724$. This implies that around 72% of the universe today is the mysterious “dark energy (Λ associated)” and the remaining 28% is matter (baryonic (ordinary) & “dark matter”).

Figure 8 displays results obtained for Ω_m by several teams over the years using different types of measurements. Our results are consistent with other Ω_m (or Ω_Λ) measurements quoted in literature. For e.g., using SNe Ia data and the same χ^2 -minimization routine followed in this study, [12] obtained (assuming flat Λ CDM cosmology): $\Omega_m, \Omega_\Lambda = 0.277^{+0.022}_{-0.022}$ (68% confidence), 0.723. Furthermore, they did not only utilize SNe Ia data but also used other measurements (H_0 , cosmic microwave background (CMB), baryon acoustic oscillations (BAO)) to put combined constraints on Ω_m . However, when combining datasets one needs to be careful since some datasets might not be completely independent of each other, in which case the results are inconsistent. For e.g., [13] mentions that supernova and BAO datasets are not entirely consistent.

In the later part of the study, opacity was inducted into our study. Analyzing how distances would be affected in a non-transparent universe, we were able to adapt our distance models to a non-transparent universe. By comparing distance moduli calculated using these updated models against distance moduli obtained from the union 2.1 SNe Ia compilation we were able to constrain Ω_m and ϵ . However, by this point we had only put constraints with SNe Ia analysis. We extended our investigation by then analyzing $H(z)$ measurements. In the last step, $H(z)$ and SNe Ia χ^2 calculations were combined to put joint constraints on Ω_m and ϵ . Marginalization over H_0 was carried out in the analysis of SNe Ia measurements but not in the analysis of $H(z)$ measurements. The resulting constraints (with marginalisation over H_0 in case of SNe Ia) are shown in figure 7 (right).

On inspecting figure 7, one can infer that joint contours seem to be centered around $\epsilon \sim -0.02$. Furthermore, the joint 3σ contours are roughly in the range $-0.06 \lesssim \epsilon \lesssim 0.04$. These findings suggest negligible opacity or equivalently, a transparent universe (to be precise, an “extremely close to” transparent universe) since these magnitudes are very close to $\epsilon = 0$. The results obtained are inline with what similar studies have concluded.

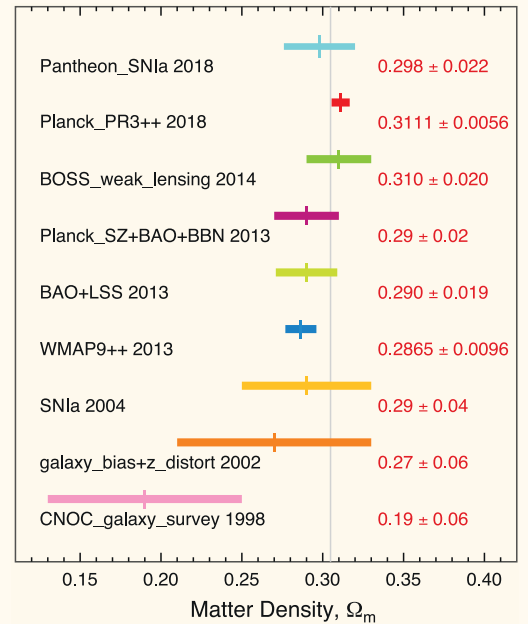


Figure 8: Determination of the mass density parameter over the years. The grey line (at $\Omega_m = 0.3049$) represents the weighted-average of WMAP and Planck data. CC: NASA/LAMBDA Archive Team.

For e.g., In [8], the authors place constraints on Ω_m and ϵ having marginalised over H_0 in analysis of both SNe Ia and $H(z)$ (assuming flat Λ CDM cosmology). They obtain $\epsilon = -0.01^{+0.08}_{-0.09}$, and their joint constraints (on ϵ & Ω_m) roughly lie in the same region in the $\Omega_m - \epsilon$ plane as ours. Authors of [19] constrain ϵ in a cosmological-model independent fashion and deduce a completely transparent universe as well. This means the expansion of the universe is in fact not being mimicked by some photon absorption mechanism, hence a non-transparent universe is ruled out.

In the 1st part of the study, rather than marginalising over H_0 to obtain $(\Omega_m)_{best}$, one could put constraints on H_0 and Ω_m both (similar to constraining ϵ & Ω_m) since $\chi^2(\mu_{theo})$ calculations were sensitive to the value of H_0 used (before marginalization, see table 1). This could be used to obtain the best-fit value of H_0 . Our analysis suggests that $H_0 \approx 70 \text{ kms}^{-1} \text{ Mpc}^{-1}$ since χ^2_{min} with $H_0 = 70 \text{ kms}^{-1} \text{ Mpc}^{-1}$ was extremely close to χ^2_{min} for $(\Omega_m)_{best}$ (~ 563 & 562 , respectively). Another way this study could be extended is by splitting Ω_m further into density parameters for baryonic and dark matter each so that density parameter of each type of matter could be constrained separately.

In the analysis of SNe Ia (for both Ω_m and ϵ) we had to resort to interpolation since we could not compute theoretical distance moduli at redshifts of the union2.1 dataset owing to processing power constraints. As mentioned in the “Method & Results” section, the redshift data was in fact not equally-spaced or uniform (see figure 9). A more precise approach would have been to compute μ_{theo} exactly at data redshifts rather than consider fewer equally-spaced (“artificial”) redshifts ($200 < 580$). Precision of constraints on $(\Omega_m)_{best}$ and ϵ could also be improved by considering more “dense” intervals for Ω_m and ϵ rather than using just 200 values for both. This would mean more smooth confidence regions in figure 7 and closer (χ^2, Ω_m) data points in figure 5, hence more precise numerical constraints on $(\Omega_m)_{best}$, i.e., no more variation in steps of 0.005 on the quoted errors in table 2.

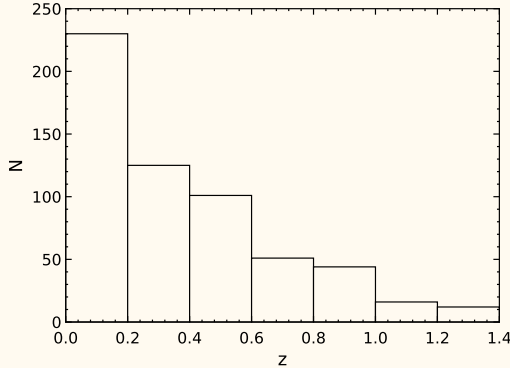


Figure 9: SNe Ia vs redshift distribution of the union2.1 SNe Ia compilation [12]. The distribution is skewed left since low-redshift distance are comparatively easier to obtain.

In constraining ϵ , the analysis of $H(z)$ was biased towards the value of H_0 used since no marginalization was carried out. This could impact the width of grey confidence bands ($H(z)$ analysis) in figure 7 since χ^2 values with marginalization could be different (recall the difference in width & placement of blue contours (SNe Ia analysis) going from (left) to (right) in figure 7). Authors of [8] placed constraints on Ω_m and ϵ having marginalised over H_0 in analysis of both SNe Ia and $H(z)$. As suggested, their confidence contours from $H(z)$ analysis in fact have different widths.

Throughout the study, a flat Λ CDM model cosmology was assumed (equations (1) and (6)). However, a more robust approach to place constraints on Ω_m and ϵ is by doing the analysis in a cosmological-model independent way. [16, 17, 18, 19] constrain cosmic opacity in a cosmological-model independent way. Furthermore, the observed distance moduli data from union2.1 sample is itself not cosmological-model independent since a value for H_0 and a cosmological model is assumed. To deal with this often the “SALT” method is used which introduces new parameters in the definition of μ (equation (3)). Using these new parameters directly instead of observed μ , one can get rid of the cosmological-model dependence in dealing with SNe Ia [20].



REFERENCES

- [1] A. Riess et al., (1998), *Observational Evidence from Supernovae for an Accelerating Universe and a Cosmological Constant*, The Astronomical Journal, <https://doi.org/10.1086%2F300499>.
- [2] S. Perlmutter et al., (1999), *Measurements of Ω and Λ from 42 High-Redshift Supernovae*, The Astrophysical Journal, <https://doi.org/10.1086%2F307221>.
- [3] C. Csáki, N. Kaloper, J. Terning, (2002), *Dimming Supernovae without Cosmic Acceleration*, Physical Review Letters, <https://doi.org/10.1103%2Fphysrevlett.88.161302>.
- [4] A. Green, (2022), *PHYS4003 Introduction to Cosmology*, University of Nottingham.
- [5] D. N. Spergel et al., (2003), *First Year Wilkinson Microwave Anisotropy Probe (WMAP) Observations: Determination of Cosmological Parameters*, The Astrophysical Journal Supplement Series, <https://doi.org/10.1086%2F377226>.
- [6] P. Ruiz-Lapuente, (2007), *Dark energy, gravitation and supernovae*, Classical and Quantum Gravity, <https://doi.org/10.1088%2F0264-9381%2F24%2F11%2F01>.
- [7] I.M.H. Etherington, (1933), *LX. On the definition of distance in general relativity*, The London, Edinburgh, and Dublin Philosophical Magazine and Journal of Science, <https://doi.org/10.1080/14786443309462220>.
- [8] A. Avgoustidis et al., (2009), *Consistency among distance measurements: transparency, BAO scale and accelerated expansion*, Journal of Cosmology and Astroparticle Physics, <https://doi.org/10.1088%2F1475-7516%2F2009%2F06%2F012>.
- [9] A. Goobar, B. Leibundgut, (2011), *Supernova Cosmology: Legacy and Future*, Annual Review of Nuclear and Particle Science, <https://doi.org/10.1146%2Fannurev-nucl-102010-130434>.
- [10] M. Hamuy et al., (1993), *The 1990 Calan/Tololo Supernova Search*, The Astronomical Journal, <https://ui.adsabs.harvard.edu/abs/1993AJ....106.2392H>.
- [11] M. Hamuy et al., (1995), *A Hubble Diagram of Distant Type 1a Supernovae*, The Astronomical Journal, <https://ui.adsabs.harvard.edu/abs/1995AJ....109....1H>.
- [12] The Supernova Cosmology Project, (2012), *The Hubble Space Telescope Cluster Supernova Survey: V. Improving the Dark Energy Constraints Above $z > 1$ and Building an Early-Type-Hosted Supernova Sample*, The Astrophysical Journal, <https://doi.org/10.1088%2F0004-637x%2F746%2F1%2F85>. Union2.1 compilation: <https://supernova.lbl.gov/Union/>.
- [13] L. Verde, (2010), *Statistical Methods in Cosmology*, https://doi.org/10.1007%2F978-3-642-10598-2_4.
- [14] G. E. Addison, G. Hinshaw, M. Halpern, (2013), *Cosmological constraints from baryon acoustic oscillations and clustering of large-scale structure*, MNRAS, <https://doi.org/10.1093%2Fmnras%2Fftt1687>.
- [15] Jun-Jie Wei, Xue-Feng Wu, (2017), *An Improved Method to Measure the Cosmic Curvature*, The Astrophysical Journal, <https://doi.org/10.3847%2F1538-4357%2Faa674b>.
- [16] K. Liao, A. Avgoustidis, Z. Li, (2015), *Is the Universe transparent?*, Physical Review D, <https://doi.org/10.1103%2Fphysrevd.92.123539>.
- [17] Yu-Bo Ma et al., (2019), *Testing Cosmic Opacity with the Combination of Strongly Lensed and Unlensed Supernova Ia*, The Astrophysical Journal, <https://doi.org/10.3847/1538-4357/ab50c4>.
- [18] K. Liao et al., (2013), *Testing cosmic opacity from SNe Ia and Hubble parameter through three cosmological-model-independent methods*, Physics Letters B, <https://doi.org/10.1016%2Fj.physletb.2012.12.022>.
- [19] Jing-Zhao Qi et al., (2019), *Cosmic opacity: Cosmological-model-independent tests from gravitational waves and Type Ia Supernova*, Physics of the Dark Universe, <https://doi.org/10.1016/j.dark.2019.100338>.
- [20] X. Yang et al., (2013), *AN IMPROVED METHOD TO TEST THE DISTANCE-DUALITY RELATION*, The Astrophysical Journal Letters, <https://dx.doi.org/10.1088/2041-8205/777/2/L24>.

APPENDIX

⇒ Luminosity distance error equation derivation:

By re-arranging equation (3) to make d_{lum} the subject, we arrive at:

$$d_{lum} = 10^{\left(\frac{\mu-25}{5}\right)}.$$

To derive δd_{lum} , start by considering the general error propagation equation which is given by:

$$(\delta A)^2 = \left(\frac{\partial A}{\partial u}\right)^2 \cdot (\delta u)^2 + \left(\frac{\partial A}{\partial v}\right)^2 \cdot (\delta v)^2 + \dots,$$

where A is a function depending on variables u, v, \dots , i.e. $A(u, v, \dots)$, and the co-efficient δ stands for uncertainty in the relevant variable/function. Applying this equation for d_{lum} , we arrive at the following equation which relates δd_{lum} to $\delta\mu$:

$$(\delta d_{lum})^2 = \left(\frac{\partial d_{lum}}{\partial \mu}\right)^2 \cdot (\delta\mu)^2,$$

where $\frac{\partial d_{lum}}{\partial \mu}$ can be calculated using the rule:

$$\frac{d}{dx} a^{f(x)} = a^{f(x)} \cdot \ln(a) \cdot \frac{df}{dx},$$

where a is a constant. Applying this rule for $\frac{\partial d_{lum}}{\partial \mu}$, we get:

$$\frac{\partial d_{lum}}{\partial \mu} = \frac{\partial}{\partial \mu} \left[10^{\left(\frac{\mu-25}{5}\right)} \right] = 10^{\left(\frac{\mu-25}{5}\right)} \cdot \ln 10 \cdot \frac{1}{5},$$

substituting this result in the equation for $(\delta d_{lum})^2$ and rearranging a bit, we obtain the following relation between δd_{lum} and $\delta\mu$:

$$\delta d_{lum} = \frac{d_{lum} \ln 10}{5} \cdot \delta\mu.$$